PRACTICAL PAPER

Improved Well Positions for Geoscientific Applications: Exploiting NAPP Photographs with Digitizer and PC-Based Bundle Adjustment Program

Robert M. Frost

Abstract

The spatial integrity of commercially available and/or proprietary digital well databases has not, in the past, been a topic of concern for many geoscientists. These data sets are used, often without question, in numerous geologic and petrophysical applications. However, as the focus and geographic extent of a given study area narrows, the need for more accurate well positions often becomes apparent. In some situations, an adequate and cost-effective solution may be achieved by using readily available and relatively inexpensive photogrammetric products and equipment (NAPP photo enlargements and digitizer) together with a robust PC-based analytical triangulation package. The procedure described below yields positions with accuracies which can approach that of the 7½-minute USGS quadrangle maps from which the necessary control coordinates are scaled.

Introduction

The oil and gas exploration and production (E&P) industry has — as have many other industries, service companies, and governmental agencies — invested significant resources towards the purchase, development, and/or implementation of some form of geographic information system. Accompanying the growth of GIS has been the development of an increasing number of commercially available and proprietary digital cartographic databases. Thappa and Bossler (1992) suggest that the quality and accuracy of a GIS database is a topic not usually discussed by developers, vendors, consultants, and end-users of GIS. They further assert that "a principal deficiency of spatial information systems is that they do not include information about the sources, quality, and accuracy of data." The systems and databases developed by and for the E&P industry are probably no exception. If, in fact, a digital data set contains information about spatial accuracy, there may be few if any systems which can convey this information in a meaningful way to end-users. As a consequence, databases developed to meet the quality requirements of a given application are often misused in other applications which require much greater spatial integrity. Whether done consciously or unwittingly, the result of such an abuse is often meaningless, is sometimes costly, and may be dangerously misleading.

Many of the data sets used by explorationists are the result of what Thappa and Bossler refer to as "secondary methods of data collection" whereby data are "collected from existing documents such as maps, charts, graphs, etc." This is commonly done with a digitizer or scanner. Because there are no rigorous standards for secondary methods of data collection, the errors present in the resultant database may vary widely, are sometimes quite gross, and often remain unknown. Even so, an explorationist interested only in mapping broad regional trends may find such a data set acceptable for his needs. However, the geologist, geophysicist, or petroleum engineer conducting narrowly focused studies over a smaller geographic area (e.g., field or reservoir-wide studies) may require significantly higher spatial accuracy, particularly with regard to well and seismic positions. To satisfy this requirement, the "primary methods of data collection" — described by Thappa and Bossler (1992) as those methods "in which data are collected directly from the field (ground surveying, photographs (aerial and terrestrial), and satellite imagery)" — are usually employed.

A "primary method" of data collection and processing is described in this paper which may yield suitably accurate well positions for many geologic and petrophysical applications. With due care and the power and sophistication of a PC-based bundle adjustment program, an optimal solution is obtained from readily available and relatively inexpensive photo products and measurement equipment: i.e., stereo pairs of NAPP photo enlargements, 7½-minute USGS quadrangle maps, and a digitizer. In addition, the results of a test case are presented along with a description of the circumstances which render this process cost-effective and desirable.

Amoco Production Company, 501 Westlake Park Boulevard, Houston, TX 77079.

Photogrammetric Engineering & Remote Sensing, Vol. 61, No. 7, July 1995, pp. 927–934.

0099-1112/95/6107–927$3.00/0

Materials, Equipment, and Software

NAPP Photo Enlargements

The objective of the National Aerial Photography Program (NAPP), according to Light (1993), is to "acquire and archive photographic coverage of the conterminous United States at 1:40,000 scale (from an altitude of 20,000 feet) using either color infrared or black-and-white film." The general public may purchase NAPP photographic products (B&W film negatives, CIR film positives, 9- by 9-inch contact prints, and up to 4× enlargements) at a reasonable cost through the EROS Data Center in Sioux Falls, South Dakota, or through the nearest National Cartographic Information Center. A more thorough description and examination of the program, its technical characteristics, and potential applications is offered by Light (1993). Some aspects relevant to this paper are cited below:

- Ground Resolution: 1.0 to 1.5 metres.
- Precision Attainable in Analytical Triangulation.
  Horizontal Position: $\delta = 0.4$m
  Vertical Position: $\delta = 0.7$m
- Allowable Enlargement Factor: 4.5×.
- Stereo Coverage: approximately 60 percent forward and 30 percent side lap.

NAPP Camera Calibration Reports

The NAPP camera calibration reports contain important technical information about the camera systems used in the NAPP program and may be obtained on request from the USGS National Mapping Division in Reston, Virginia. Data used in the procedure described in this paper are

- Radial lens distortion expressed in µm for given field angles,
- Calibrated focal length,
- Calibrated fiducial coordinates (the fiducials are reference points fixed in the camera body, usually at the corners and/or sides of the focal plane opening, and are imaged on each photo. Lines joining opposite fiducials intersect at a point which serves as the origin of a photo centered *xy* coordinate system and is the system in which the fiducials themselves are defined (Wolf, 1983). This origin very nearly coincides with the calibrated principal point), and
- Calibrated principal point (the calibrated principal point coordinates reflect the location of the point of photographic symmetry with respect to the fiducial coordinate system described above).

USGS 7½-Minute Topographic Quadrangle Maps

The U.S. Geological Survey produces and makes available to the general public a wide variety of topographic, geologic, and geophysical map products in both digital and hard copy format. One of the most widely used products is the 7½-minute topographic quadrangle map. These 1:24,000-scale maps comply with National Map Accuracy Standards. In terms of horizontal accuracy, this standard requires that, for maps at scales of 1:20,000 or smaller, not more than 10 percent of well-defined features be in error by more than 1/50 inch (equivalent to 40 feet at ground scale for the 7½-minute topographic maps). The vertical accuracy standard applied to all publication scales requires that not more than 10 percent of elevations tested be in error by more than one-half the contour interval (ACSM/ASCE, 1978).

Summagraphics Microgrid III Series Digitizer

The Microgrid III digitizer is an input device which can capture graphic information from drawings, photographs, etc., and translate that information into computer readable format. Positions are expressed as *xy* coordinate pairs which can be written to a digital data file. Some relevant performance characteristics from the user's manual are

- Resolution: up to 2000 lines per inch.
- Accuracy: ± 0.002 to 0.005 inches (50 to 127 µm).
- Repeatability: ± 0.002 inches (50 µm).

This digitizer is not in the same class of photogrammetric measuring devices as, say, a 2-µm monocomparator. But, it can deliver 50- to 127-µm accuracy, which is adequate for this application (in addition to the fact that this and similar digitizers are, comparatively speaking, inexpensive and commonly found in businesses engaged in any form of mapping).

PC Giant 1990, GPA Associates — PC-Based Bundle Adjustment Program

PC Giant is a "complete photogrammetric system" consisting of the main triangulation program, various preprocessing routines, several tools which facilitate the graphic analysis of adjustment runs, along with utilities which can perform supporting operations such as the direct or inverse transformation between geographic and grid coordinates. The triangulation program "will perform a simultaneous bundle adjustment of perspective imagery (photos, X-rays, etc.) by enforcing the collinearity condition" and "can optionally perform an error propagation analysis of the geometric dilution of precision (GDOP) for every point in the adjustment, including pass points." This program enables the user to differentially weight input data and can express the object space in either a geographic or rectangular coordinate system. For the application described in this paper, it is assumed that a relatively few photos are involved. However, this program can operate on a "virtually unlimited" number of photographs. (The information above was excerpted from the PC-Giant user's manual.)

Procedure

Overview

The procedure involves identifying, verifying, and marking on the photos the wells or other points of interest, along with various control points. These control points, usually road intersections, are also identified on the topographic maps from which their horizontal coordinates and elevations are scaled. Next, all relevant points (wells, control, fiducials) are digitized from the photos. These data are reformatted and submitted, together with information contained in the camera calibration report, to PC Giant. Following various preprocessing functions, the program then simultaneously performs a resection to solve for the position and orientation of the camera stations, and triangulation to determine the positions of the wells (or other selected pass-points). A visual representation of the resection and triangulation is shown in Figure 1.

Identifying and Marking Points of Interest

The quality and resolution of 4× NAPP photo enlargements is such that oil well pumping units, and in particular the pump-jack shadows, are easily discernable. From this, well locations may be easily spotted and marked with a small pin prick on each photo in which they appear (each well must appear in a minimum of two photos). The location of a gas or injection well is not as easily spotted because the attendant well equipment is, usually, physically smaller. If this is the case, the assistance of a drilling engineer might prove

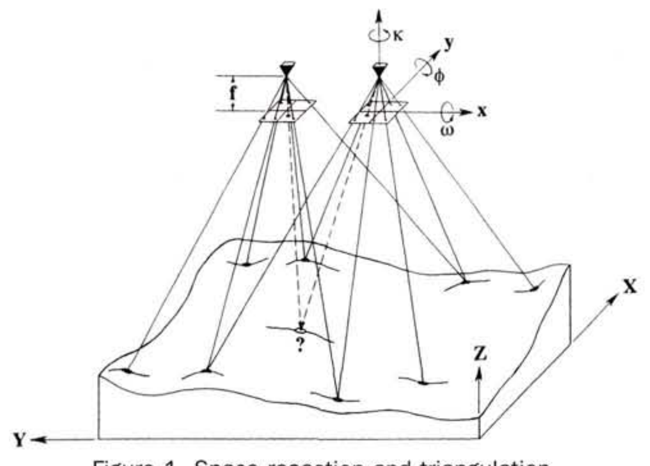

Figure 1. Space resection and triangulation.

very helpful. If there is any doubt, his knowledge of drilling practices, pad design, and construction in the area of interest could result in a much more accurate pick.

Associating a well name or identifier with a photo pick will almost certainly require the use of ancillary data. A good source of these data is the state regulatory agency responsible for providing drilling permits. These regulatory agencies are in place primarily to enforce drilling and spacing requirements which, in turn, help ensure public safety and prevent wasteful exploration and production practices. The permit plats submitted by operating companies usually depict the proposed well location and well name; distances to appropriate lease, regulatory, and/or other land boundaries; distances to nearby wells; and in some cases an acreage assignment or "proration unit." However, the absolute position of the proposed well (expressed as a geographic or grid coordinate) is often not required by the regulatory agency or disclosed on the plat. Nevertheless, the permit plats are part of the public record, are easily accessed, and usually show a sufficient amount of detail so that a well name or identifier can be readily associated with a well visible on an NAPP photo.

A well-distributed set of control points (e.g., road intersections) is also selected and marked on the photos. For this procedure, a minimum of four control points per photo is used. (Because of this, a least-squares space resection could actually be performed for each photo independently. The author has not attempted a solution which "bridges" through a strip or block of photos. The areas of interest, thus far encountered, have usually been limited such that one or two NAPP stereo models provide sufficient coverage.) The selected control points are then identified and marked on the appropriate 7½-minute topographic maps.

Identifying, verifying, and marking the features of interest is probably the most tedious and time-consuming part of the overall procedure. However — aside from being a prerequisite to a good final solution — the care and effort invested here will enable the measurement process to proceed relatively quickly.

Photo and Map Measurements

Having identified and marked the features of interest, each photo is secured to the digitizing tablet and the wells, control points, and fiducials are all carefully digitized. Each photo is digitized separately and the coordinates and point identifiers are written out to an ASCII file. The rectangular coordinate system used for each photo may be arbitrarily defined or may reflect the absolute system of the digitizing tablet. The aim here is to capture coordinate values in *some* rectangular system at the full precision of the digitizer. Avoid using digitizing algorithms which require the use of more than two points for set-up (these programs sometimes perform affine, non-orthogonal, or projective coordinate transformations which, for this measurement process, may introduce unwanted error).

The object space coordinates of the control points are determined thus: The USGS 7½-minute topographic maps have, along the border, grid ticks which are usually marked at 10,000-foot intervals. These "ticks" may serve as reference marks for determining the horizontal position of the control points in the designated state-plane coordinate system (e.g., Texas South Central Zone, Louisiana North Zone, etc.). A long straight edge is used to very carefully draw lines joining corresponding grid ticks on opposite sides of the topographic map. An engineer's scale is then used to carefully measure the *XY* coordinates of the control points (estimated to the nearest 10 feet). If road intersections are chosen for control, they will often have spot elevations, expressed to the nearest foot, indicated on the topographic map. If not, elevations need to be interpolated from the contour lines.

Preprocessing

Most of the preprocessing functions are designed to reduce the measured photo coordinates to a photo-centered coordinate system and to remove a variety of systematic errors. Wolf (1983) describes the major sources of error as lens distortion, shrinkage and expansion of photo material, principal point offset, atmospheric refraction, and Earth curvature.

PC Giant can calculate the coefficients of radial lens distortion from data contained in the camera calibration report. However, the lens distortions of the NAPP camera systems encountered thus far are, for this application, negligible. Nevertheless, as a matter of good practice, and in the event a system is encountered which has significant lens distortion, this processing step should be carried out.

All measured photo coordinates are reduced to a plate- or photo-centered coordinate system through a PC Giant preprocessing routine, PREP, which can generate the coefficients of, and apply, an eight-parameter projective coordinate transformation based on the calibrated fiducial coordinates and their corresponding measured values. In addition, this transformation accounts for film shrinkage and expansion (and, to some degree, distortions introduced in the enlargement process). The calibrated principal point offset indicated in the camera calibration report may also be input and accounted for. Corrections for radial lens distortion are then performed (assuming the coefficients were calculated and supplied to PREP).

The control point data captured from the 7½-minute topographic maps are in the form of state plane coordinate *XY*s and elevations. So that the program can account for Earth curvature, these data should be transformed into latitude, longitude, and ellipsoid height (for this application, elevation and ellipsoid height are considered equivalent).

Following these preprocessing steps, the data are ready for reformatting into two files which will serve as input for the main triangulation run. The first file contains the photo identifier, calibrated focal length, *a priori* estimates of stan-

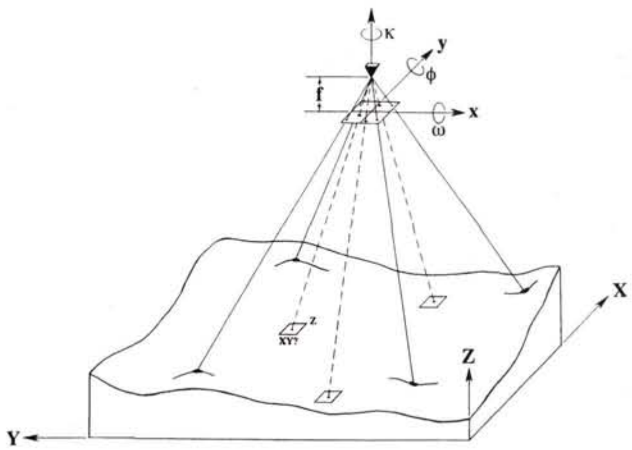

Figure 2. Differential single ray.

dard deviations for the image *xy* coordinates, and the image *xy* coordinates with identifiers (on a photo-by-photo basis). The second file contains estimates of camera position and orientation for each frame. These estimates can be quite gross and the *a priori* standard deviations assigned should reflect this. This file also contains a listing of the latitude, longitude, and height of every control point, together with the respective point identifiers and an *a priori* estimate of standard deviation for each positional component.

Triangulation

The purpose of a "bundle" adjustment, according to Wolf (1983) is "to adjust all photogrammetric measurements to ground control values in a single solution." PC Giant performs this function by enforcing the collinearity condition. Again, quoting from Wolf, "Collinearity ... is the condition that the exposure station, any object point, and its photo image all lie along a straight line. Two equations express the collinearity condition for any point on a photo: one equation for the *x* photocoordinate and another for the *y* photocoordinate, i.e.,

$$x = -f[m_{11}(X - X_L) + m_{12}(Y - Y_L) + m_{13}(Z - Z_L) / m_{31}(X - X_L) + m_{32}(Y - Y_L) + m_{33}(Z - Z_L)] \quad (1)$$

$$y = -f[m_{21}(X - X_L) + m_{22}(Y - Y_L) + m_{23}(Z - Z_L) / m_{31}(X - X_L) + m_{32}(Y - Y_L) + m_{33}(Z - Z_L)] \quad (2)$$

where x and y are photo coordinates of an image point; X, Y, and Z are ground coordinates of the object point; X_L, Y_L, and Z_L are ground coordinates of the exposure station; f is the camera focal length; and the m's are functions of the rotation angles omega [ω], phi [ϕ], and kappa [κ]." (Note that the PC Giant triangulation program internally converts the control point's latitude, longitude, and ellipsoid height to geocentric X, Y, and Z for processing. All geocentric X, Y, and Z coordinates derived in the adjustment are converted to latitude, longitude, and ellipsoid height for final output.)

The input files submitted to the bundle adjustment routine contain the information necessary for an iterative least-squares solution which enforces the collinearity condition and simultaneously computes the position and orientation of the camera stations and the object space coordinates of any unknown point appearing in a minimum of two overlapping photos (refer to Figure 1). All positional information and residual data, along with an error propagation of the geometric dilution of precision for every point, are output in ASCII format to hard disk files.

As an aside, it is possible to calculate the horizontal position of a point which appears in only one photo, provided its elevation is known (Mugnier, 1978). The horizontal positions of any number of points with known elevations could be solved for in a single photo process of differential single-ray. Conceptually, rays emanating from an exposure station — whose position and orientation in object space are known — are passed through points in the photo image plane, and are intersected with planes fixed at the elevations of the corresponding ground points (see Figure 2). This can be accommodated in PC Giant by including, in the control point file, gross estimates for the unknown horizontal positions (weighted accordingly) along with their known elevations which are constrained very tightly (*a priori* standard deviation of zero).

Post Processing

Following the triangulation run, a post adjustment analysis may be performed. PC Giant provides some useful tools for the graphical display and analysis of plate residuals and the error ellipsoids computed for each ground point. The estimated standard deviations of all object space coordinates should also be examined.

Many, if not all, of the ground points may be determined from two-ray intersections (a circumstance which is usually avoided in actual photogrammetric practice). Associated plate residuals, especially for two-ray points, will tend to become zero in the direction of flight as the error resolves itself in the vertical component. This should be watched carefully. Otherwise, residuals should more or less balance for each point and, as a whole, conform to the laws of normal distribution.

The positions and orientations of a series of exposure stations should normally reflect the consistent path of an aircraft flying, more or less, straight and level. Also, the *a posteriori* estimate of variance of unit weight, which reflects the balance between input standard deviations and output residuals, should approach one (1) if realistic weights were used. (The above was excerpted from the PC Giant user's manual. In the event the solution fails to converge, this manual offers information about editing strategies which can help to identify and rectify blunders.)

Test Case

General Information

A suitable portion of an Amoco operated field in West Texas was selected for this study. The area has an average elevation of 3600 feet and low to moderate relief. Using the procedure described above, the horizontal and vertical positions were determined for 22 oil wells which appear in the overlap area of two consecutive black-and-white NAPP photos. The pumping units and pump-jack shadows are clearly visible in these photos which were taken in January, 1991. A total of nine control points was used: six appear in one photo, seven in the other. The results of this test are evaluated against the state plane coordinates and elevations of the wells as previously determined by actual field surveys.

The *a priori* standard deviation used to weight measured photo coordinates was 50 μm. This estimate (an adjusted value which reflects the refinement gained from working

TABLE 1. EIGHT-PARAMETER RESIDUALS OF FIDUCIAL COORDINATES (MM)

Frame 3348-00A			Frame 3348-00B		
Fid	X	Y	Fid	X	Y
1	−0.017	−0.049	1	−0.020	−0.030
2	0.048	0.021	2	0.049	0.007
3	−0.027	0.018	3	−0.032	0.030
4	0.018	−0.088	4	0.050	0.027
5	0.020	−0.007	5	0.043	0.027
6	−0.082	−0.015	6	−0.097	−0.008
7	0.010	−0.020	7	0.010	−0.063
8	0.030	0.139	8	−0.002	0.011
Rms	0.038	0.062	Rms	0.047	0.031

TABLE 2. TRIANGULATED IMAGE POINT RESIDUALS FOR CONTROL POINTS (μM)

Point ID	Frame-ID X Y	Frame-ID X Y	Point ID	Frame-ID X Y
C9	3348-00A	3348-00B	C6	3348-00A
	18	−14		−2
	−23	19		−2
C8	3348-00A	3348-00B	C7	3348-00A
	−18	15		4
	−1	−3		−6
C4	3348-00B	3348-00A	C1	3348-00B
	−26	18		10
	12	−7		0
C5	3348-00B	3348-00A	C2	3348-00B
	19	−21		2
	−17	16		8
			C3	3348-00B
				−6
				3

with 4× enlargements) was based on the specified accuracy of the Summagraphics Microgrid III digitizer and is supported somewhat by the RMSs of the residuals generated in the eight-parameter PREP transformations shown in Table 1.

The *a priori* standard deviation used to weight the object space control was 0.30 seconds in longitude and 0.25 seconds in latitude, which equates to about 25 feet in X and Y grid coordinates. This estimate is based on the relationship between the National Map Accuracy Standard 90 percent Circular Map Error (applicable to USGS 7½-minute topographic maps) and the corresponding standard deviation in X or Y. This relationship is given in the "ASPRS Accuracy Standards for Large-Scale Maps" (ASPRS, 1990) and is as follows:

$$\text{90\% Circular Map Error} = 2.146\ \delta_x = 2.146\ \delta_y. \tag{3}$$

Therefore, for a 7½-minute topographic map, the 90 percent Circular Map Error of 40 feet equates to a standard deviation in X or Y of about 20 feet. The elevations of the object space control were assigned an *a priori* standard deviation of 1 foot, as spot elevations, expressed to the nearest foot, were available from the topos.

Results

Following the previously described data collection and preprocessing procedures, a complete triangulation run was attempted and successfully converged in five iterations. The results of the triangulation and requested error propagation were output by PC-Giant to several files from which the following tables are excerpted.

The resultant *a posteriori* variance of unit weight was 0.3, which might indicate that the *a priori* standard deviations, were too large (or overly pessimistic). An examination of Table 2 reveals that the image point residuals are well balanced and significantly less than 50 μm. Also, the standard

TABLE 3. TRIANGULATED CONTROL POINT COVARIANCE MATRICES AND STANDARD DEVIATIONS.

Ident	Covariance Matrix				Std Dev
	+2.668E−13	+1.490E−14	−1.254E−09	Lng	00 00 0.1065
C3	+1.490E−14	+1.623E−13	−1.238E−09	Lat	00 00 0.0831
	−1.254E−09	−1.238E−09	+2.573E−02	Elv(m)	0.1604
	+1.869E−13	−3.148E−15	+9.977E−10	Lng	00 00 0.0892
C2	−3.148E−15	+1.236E−13	−1.517E−09	Lat	00 00 0.0725
	+9.977E−10	−1.517E−09	+2.573E−02	Elv(m)	0.1604
	+2.252E−13	−9.265E−15	+2.088E−09	Lng	00 00 0.0979
C1	−9.265E−15	+1.325E−13	−9.697E−10	Lat	00 00 0.0751
	+2.088E−09	−9.697E−10	+2.573E−02	Elv(m)	0.1604
	+2.671E−13	−1.629E−14	−1.142E−09	Lng	00 00 0.1066
C7	−1.629E−14	+1.948E−13	+1.063E−09	Lat	00 00 0.0910
	−1.142E−09	+1.063E−09	+2.573E−02	Elv(m)	0.1604
	+2.664E−13	+1.102E−14	+1.802E−09	Lng	00 00 0.1065
C6	+1.102E−14	+1.590E−13	+9.977E−10	Lat	00 00 0.0822
	+1.802E−09	+9.977E−10	+2.573E−02	Elv(m)	0.1604
	+1.431E−13	+1.772E−17	+1.719E−09	Lng	00 00 0.0780
C5	+1.772E−17	+9.903E−14	+8.127E−10	Lat	00 00 0.0649
	+1.719E−09	+8.127E−10	+2.570E−02	Elv(m)	0.1603
	+1.658E−13	+4.914E−15	−1.625E−09	Lng	00 00 0.0840
C4	+4.914E−15	+1.200E−13	+5.427E−10	Lat	00 00 0.0715
	−1.625E−09	+5.427E−10	+2.571E−02	Elv(m)	0.1604
	+1.278E−13	−7.854E−15	−1.129E−09	Lng	00 00 0.0738
C8	−7.854E−15	+9.876E−14	−8.745E−10	Lat	00 00 0.0648
	−1.129E−09	−8.745E−10	+2.571E−02	Elv(m)	0.1603
	+1.354E−13	+1.072E−15	+2.393E−09	Lng	00 00 0.0759
C9	+1.072E−15	+9.297E−14	−3.117E−10	Lat	00 00 0.0629
	+2.393E−09	−3.117E−10	+2.569E−02	Elv(m)	0.1603

TABLE 4. TRIANGULATED CAMERA STATIONS

Ident	Position	Error Ellipsoid	→	Length
	Lng = −102 35 30.3963	−0.9663 +0.2234 +0.1275	→	5.5851m
3348−00A	Lat = 33 26 14.5407	−0.2408 −0.9600 −0.1426	→	4.5301m
	Elv = 7289.8938	+0.0906 −0.1685 +0.9815	→	1.9714m
	Omega = − 01 13 13.0657	00 01 52.6524		
	Phi = − 01 00 37.9944	Std. Dev. 00 01 56.1779		
	Kappa = − 89 07 15.2536	00 01 3.5448		
	Lng = −102 35 26.4325	+0.1904 +0.9675 −0.1666	→	4.7138m
3348−00B	Lat = 33 28 11.8959	+0.9813 −0.1926 +0.0029	→	4.6801m
	Elv = 7288.3385	−0.0293 −0.1641 −0.9860	→	1.9129m
	Omega = − 00 29 22.4248	00 01 35.5919		
	Phi = 00 10 47.5190	Std. Dev. 00 01 57.6198		
	Kappa = − 89 52 50.2363	00 01 2.0575		

deviations of the triangulated control points, shown in Table 3, are roughly one-third to one-half their *a priori* estimates. This supports the notion that, for this example, a heavier weighting may have been appropriate.

The flight paths for NAPP photography are oriented generally north-south. The triangulated camera stations in Table 4 show that these two photos were taken from an aircraft flying basically straight and level and from south to north. The positive *x* axis of the camera system, for this example, corresponds with the direction of flight; hence, the yaw angle (κ) from the photo to ground coordinate system is roughly −90 degrees.

All of the well positions are the result of two-ray intersections. As expected, the *x* residuals have tended toward zero while the *y* residuals are well balanced and all within 50 μm (see Table 5). The standard deviations in latitude and longitude of the triangulated wells (see Table 6) are quite consistent, with an RMS of 0.07 seconds in latitude and 0.10 seconds in longitude (approximately 7 and 8 feet in respec-

TABLE 5. TRIANGULATED IMAGE POINT RESIDUALS FOR WELLS (μM)

Point ID	Frame−ID X Y	Frame−ID X Y	Point ID	Frame−ID X Y	Frame−ID X Y
IS20	3348−00A	3348−00B	CM208	3348−00A	3348−00B
	0	0		0	0
	0	0		−12	12
IS74	3348−00A	3348−00B	CM204	3348−00A	3348−00B
	0	0		0	0
	22	−22		8	−8
IS18	3348−00A	3348−00B	CM213	3348−00A	3348−00B
	0	0		0	0
	6	−6		−3	3
IS13A	3348−00A	3348−00B	CM205	3348−00A	3348−00B
	0	0		0	0
	19	−19		0	0
IS14	3348−00A	3348−00B	CM72	3348−00A	3348−00B
	0	0		0	0
	−10	10		−2	2
IS69	3348−00A	3348−00B	CM91	3348−00A	3348−00B
	0	0		0	0
	−21	21		23	−23
BM5	3348−00A	3348−00B	CM236	3348−00A	3348−00B
	0	0		0	0
	−15	15		−5	5
BM7	3348−00A	3348−00B	CM228	3348−00A	3348−00B
	0	0		0	0
	8	−8		−2	2
CM47	3348−00A	3348−00B	CM123	3348−00A	3348−00B
	0	0		0	0
	−5	5		−25	26
CM234	3348−00A	3348−00B	CM121	3348−00A	3348−00B
	0	0		0	−1
	13	−13		43	−43
CM52	3348−00A	3348−00B	CM119	3348−00A	3348−00B
	0	0		0	−0
	−26	27		12	−12

TABLE 6. TRIANGULATED WELL COVARIANCE MATRICES AND STANDARD DEVIATIONS

Ident	Covariance Matrix			Std Dev	
	+1.565E−13	−1.791E−14	−4.559E−07	Lng	00 00 0.0816
CM119	−1.791E−14	+1.281E−13	+5.847E−07	Lat	00 00 0.0738
	−4.559E−07	+5.847E−07	+1.070E+01	Elv(m)	3.2713
	+1.960E−13	−3.140E−14	−7.400E−07	Lng	00 00 0.0913
CM121	−3.140E−14	+1.397E−13	+6.064E−07	Lat	00 00 0.0771
	−7.400E−07	+6.064E−07	+1.155E+01	Elv(m)	3.3987
	+2.611E−13	−4.793E−14	−1.058E−06	Lng	00 00 0.1054
CM123	−4.793E−14	+1.547E−13	+6.304E−07	Lat	00 00 0.0811
	−1.058E−06	+6.304E−07	+1.259E+01	Elv(m)	3.5488
	+2.911E−13	−4.187E−14	−1.176E−06	Lng	00 00 0.1113
CM228	−4.187E−14	+1.472E−13	+4.885E−07	Lat	00 00 0.0791
	−1.176E−06	+4.885E−07	+1.223E+01	Elv(m)	3.4966
	+2.148E−13	−2.919E−14	−8.628E−07	Lng	00 00 0.0956
CM236	−2.919E−14	+1.316E−13	+4.751E−07	Lat	00 00 0.0748
	−8.628E−07	+4.751E−07	+1.119E+01	Elv(m)	3.3458
	+1.464E−13	−1.105E−14	−4.644E−07	Lng	00 00 0.0789
CM91	−1.105E−14	+1.048E−13	+3.356E−07	Lat	00 00 0.0668
	−4.644E−07	+3.356E−07	+9.596E+00	Elv(m)	3.0978
	+1.398E−13	−3.887E−15	−4.624E−07	Lng	00 00 0.0771
CM72	−3.887E−15	+9.388E−14	+9.465E−08	Lat	00 00 0.0632
	−4.624E−07	+9.465E−08	+9.076E+00	Elv(m)	3.0126
	+1.987E−13	+1.907E−15	−8.247E−07	Lng	00 00 0.0919
CM205	+1.907E−15	+1.101E−13	−1.243E−08	Lat	00 00 0.0685
	−8.247E−07	−1.243E−08	+9.753E+00	Elv(m)	3.1229
	+1.811E−13	+9.361E−15	−7.374E−07	Lng	00 00 0.0878
CM213	+9.361E−15	+1.091E−13	−1.669E−07	Lat	00 00 0.0681
	−7.374E−07	−1.669E−07	+9.610E+00	Elv(m)	3.1000
	+1.428E−13	+4.867E−15	−4.973E−07	Lng	00 00 0.0780
CM204	+4.867E−15	+9.775E−14	−1.749E−07	Lat	00 00 0.0645
	−4.973E−07	−1.749E−07	+9.117E+00	Elv(m)	3.0194
	+1.534E−13	+8.907E−15	−5.683E−07	Lng	00 00 0.0808
CM208	+8.907E−15	+1.041E−13	−2.440E−07	Lat	00 00 0.0666
	−5.683E−07	−2.440E−07	+9.355E+00	Elv(m)	3.0586

Ident	Covariance Matrix			Std Dev	
	+1.411E−13	+9.745E−15	−4.573E−07	Lng	00 00 0.0775
CM52	+9.745E−15	+1.066E−13	−3.627E−07	Lat	00 00 0.0674
	−4.573E−07	−3.627E−07	+9.487E+00	Elv(m)	3.0801
	+1.610E−13	+1.753E−14	−5.890E−07	Lng	00 00 0.0828
CM234	+1.753E−14	+1.198E−13	−4.562E−07	Lat	00 00 0.0714
	−5.890E−07	−4.562E−07	+1.025E+01	Elv(m)	3.2021
	+1.641E−13	+1.927E−14	−6.032E−07	Lng	00 00 0.0835
CM47	+1.927E−14	+1.233E−13	−4.891E−07	Lat	00 00 0.0724
	−6.032E−07	−4.891E−07	+1.048E+01	Elv(m)	3.2370
	+2.270E−13	−1.066E−14	+1.052E−06	Lng	00 00 0.0983
BM7	−1.066E−14	+8.934E−14	−1.092E−07	Lat	00 00 0.0617
	+1.052E−06	−1.092E−07	+9.983E+00	Elv(m)	3.1596
	+2.900E−13	−1.281E−14	+1.292E−06	Lng	00 00 0.1111
BM5	−1.281E−14	+9.705E−14	−1.159E−07	Lat	00 00 0.0643
	+1.292E−06	−1.159E−07	+1.069E+01	Elv(m)	3.2690
	+2.671E−13	−2.705E−14	+1.231E−06	Lng	00 00 0.1066
IS69	−2.705E−14	+9.816E−14	−2.544E−07	Lat	00 00 0.0646
	+1.231E−06	−2.544E−07	+1.087E+01	Elv(m)	3.2970
	+2.793E−13	−3.311E−14	+1.282E−06	Lng	00 00 0.1090
IS14	−3.311E−14	+1.019E−13	−3.023E−07	Lat	00 00 0.0658
	+1.282E−06	−3.023E−07	+1.118E+01	Elv(m)	3.3439
	+2.592E−13	−5.244E−14	+1.225E−06	Lng	00 00 0.1050
IS13A	−5.244E−14	+1.154E−13	−5.198E−07	Lat	00 00 0.0701
	+1.225E−06	−5.198E−07	+1.189E+01	Elv(m)	3.4477
	+2.855E−13	−5.998E−14	+1.333E−06	Lng	00 00 0.1102
IS18	−5.998E−14	+1.216E−13	−5.537E−07	Lat	00 00 0.0719
	+1.333E−06	−5.537E−07	+1.243E+01	Elv(m)	3.5251
	+2.977E−13	−6.585E−14	+1.384E−06	Lng	00 00 0.1125
IS74	−6.585E−14	+1.268E−13	−5.922E−07	Lat	00 00 0.0734
	+1.384E−06	−5.922E−07	+1.281E+01	Elv(m)	3.5794
	+2.660E−13	−7.206E−14	+1.267E−06	Lng	00 00 0.1064
IS20	−7.206E−14	+1.390E−13	−7.295E−07	Lat	00 00 0.0769
	+1.267E−06	−7.295E−07	+1.320E+01	Elv(m)	3.6334

RMS For Standard Deviations

Count = 22	Lng = 00 00 0.0955	(approx. 8 ft)
Count = 22	Lat = 00 00 0.0704	(approx. 7 ft)
Count = 22	Elv = 3.2894 m	(approx. 11 ft)

tive ground units). The RMS for standard deviations of the elevations is about 11 feet. This is an order of magnitude larger than that of the control points. Because errors in the measured photo coordinates in the direction of flight tend to resolve themselves in the vertical ground component, this result is not surprising.

Finally, the triangulated well positions were compared to the actual well positions as determined by recent field surveys. The results are shown in Table 7. An obvious bias in the *Y* component may be due to some unaccounted-for systematic error. Even so, the results of the triangulation compare very favorably with ground truth and demonstrate that accuracies "which approach that of well-defined points measured from USGS 7½-minute topographic maps" are attainable.

Conclusion

Digital well databases generated through secondary methods of data collection may contain spatial errors which render them unfit for many applications. Errors in the positions of wells, from a few hundred to many thousands of feet and beyond, have been observed in several such databases. Confronted with uncertainty about the spatial integrity of a given digital database, geoscientists have commonly resorted to one of the following:

- Accept the data as correct. Make no attempt at improvement.
- Digitize well positions directly from aerial photographs or satellite imagery. (Numerous systematic errors and distortions, especially relief displacement, go unaccounted for. Even with exceptional operator care, this may result in significant positional inaccuracies.)
- Conduct a field survey to "tie-in" the desired wells. (Without a doubt, field surveys will almost always yield the most certain and accurate results. Time and money permitting, this would be the preferred option.)

The procedure outlined in this paper may serve as an adequate and cost-effective alternative when

- Accuracy requirements are approximately equal to that of well defined points on a 7½-minute topographic quadrangle map,
- The resolution and inherent distortion of available aerial photography and satellite imagery are such that the required accuracy cannot be attained through standard digitizing processes, and
- The cost in time and money for a field survey is prohibitive

TABLE 7. RESIDUALS OF TRIANGULATED MINUS (−) SURVEYED WELL POSITIONS (FEET)

ID	X	Y	Elev.
CM119	−0.07	−10.07	−9.3
CM121	−3.53	−9.40	−16.8
CM123	−3.75	−4.55	−1.9
CM228	−6.55	−9.49	1.8
CM236	−6.73	−10.42	−6.2
CM91	−7.71	−6.80	3.9
CM72	−6.39	−10.88	5.8
CM205	−11.96	−9.78	11.4
CM213	−6.18	−11.82	1.9
CM204	−11.89	−12.72	−2.1
CM208	−7.70	−12.51	7.2
CM52	−9.17	−14.61	5.6
CM234	−9.15	−10.94	−2.2
CM47	−11.28	−12.70	5.5
BM7	0.44	−11.83	−15.1
BM5	2.40	−18.31	−13.2
IS69	5.29	−15.89	−15.3
IS14	4.10	−20.84	−10.4
IS13A	8.76	−20.65	−8.7
IS18	3.32	−17.01	−7.3
IS74	5.83	−19.40	−11.4
IS20	10.52	−21.26	5.4
RMS	7.3	14.0	8.9

and/or the wells or other points of interest are physically inaccessible.

Acknowledgments

Amoco Production Company expressly disclaims any and all representations or warranties, express or implied, as to the accuracy, quality, or completeness of information contained in this paper, and makes no endorsement of any products or processes mentioned. I wish to acknowledge, however, the assistance and encouragement provided by the company.

References

ACSM and ASCE, 1978. *Definitions of Surveying and Associated Terms*, ACSM and ASCE, 210 p.

ASPRS, 1990. ASPRS Accuracy Standards for Large-Scale Maps, *Photogrammetric Engineering & Remote Sensing*, 56(7):1068–1070.

Light, D., 1993. The National Aerial Photography Program as a Geographic Information System Resources, *Photogrammetric Engineering & Remote Sensing*, 59(1):61–65.

Mugnier, C., 1978. Analytical Rectification Using Artificial Points, *Photogrammetric Engineering & Remote Sensing*, 44(5):579–583.

Thappa, K., and J. Bossler, 1992. Accuracy of Spatial Data Used in Geographic Information Systems, *Photogrammetric Engineering & Remote Sensing*, 58(6):835–841.

Wolf, P., 1983. *Elements of Photogrammetry*, McGraw-Hill, Inc., 628 p.

(Received 13 December 1993; accepted 7 March 1994)

Robert M. Frost

Robert holds a B.S. in Surveying and Mapping Technology from the University of Houston and has been licensed as a Professional Land Surveyor in the State of Louisiana since 1987. He has been active in the field of surveying and mapping during the last 14 years and is currently employed by Amoco Production Company as a Positioning and Navigation Specialist.

FORTHCOMING ARTICLES

B. Brisco and *R. J. Brown*, Multi-Date SAR/TM Synergism for Crop Classification in Western Canada.

Jorge Antonio Silva Centeno and *Victor Haertel*, Adaptive Low-Pass Fuzzy Filter for Noise Removal.

S. M. de Jong and *P. A. Burrough*, A Fractal Approach to the Classification of Mediterranean Vegetation Types in Remotely Sensed Images.

John L. Dwyer, *Fred A. Kruse*, and *Adam B. Lefkoff*, Effects of Empirical versus Model-Based Reflectance Calibration on Automated Analysis of Imaging Spectrometer Data: A Case Study from the Drum Mountains, Utah.

Christopher D. Elvidge, *Ding Yuan*, *Ridgeway D. Weerackoon*, and *Ross S. Lunetta*, Relative Radiometric Normalization of Landsat Multispectral Scanner (MSS) Data Using an Automatic Scattergram -- Controlled Regression.

Peng Gong, *Ruiliang Pu*, and *John R. Miller*, Coniferous Forest Leaf Area Index Estimation along the Oregon Transect Using Compact Airborne Spectrographic Imager Data.

Paul M. Harris and *Stephen J. Ventura*, The Integration of Geographic Data with Remotely Sensed Imagery to Improve Classification in an Urban Area.

Jussi Lammi and *Tapani Sarjakoski*, Image Compression by the JPEG Algorithm.

Christopher T. Lee and *Stuart E. Marsh*, The Use of Archival Landsat MSS and Ancillary Data in a GIS Environment to Map Historical Change in an Urban Riparian Habitat.

C. Leprieur, *V. Carrere*, and *X. F. Gu*, Atmospheric Corrections and Ground Reflectance Retrieval for Airborne Visible/Infrared Imaging Spectrometer (AVIRIS) Data -- MAC Europe '91.

Donald E. Luman and *Minhe Ji*, The Lake Michigan Ozone Study: An Application of Satellite-Based Land-Use and Land-Cover Mapping to Large-Area Emissions Inventory Analysis.

C. Mack, *S.E. Marsh*, and *C.F. Hutchinson*, Application of Aerial Photography and GIS Techniques in the Development of a Historical Perspective of Environmental Hazards at the Rural-Urban Fringe.

Michel Massart, *Marie Pétillon*, and *Eléonore Wolff*, The Impact of an Agricultural Development Project on a Tropical Forest Environment: The Case of Shaba (Zaïre).

Janet E. Nichol, Monitoring Tropical Rain Forest Microclimate.

K. Olaf Niemann, Remote Sensing of Forest Stand Age Using Airborne Spectrometer Data.

Stephen A. Sader, Spatial Characteristics of Forest Clearing and Vegetation Regrowth as Detected by Landsat Thematic Mapper Imagery.

Tian-Yuan Shih, The Reversibility of Six Geometric Color Spaces.

William L. Teng, *Paul C. Doraiswamy*, and *James R. Wang*, Temporal Variations of the Microwave Polarization Difference Index and Its Relationship to the Normalized Difference Vegetation Index in a Densely Cropped Area.

Michael E. Wehde, Digital Image Comparison by Subtracting Contextual Transformations: Percentile Rank Order Differentiation.

Peter T. Wolter, *David J. Mladenoff*, *George E. Host*, and *Thomas R. Crow*, Improved Forest Classification in the Northern Lake States Using Multi-Temporal Landsat Imagery.